IEEE Access
Multidisciplinary ⋮ Rapid Review ⋮ Open Access Journal

Received 19 September 2022, accepted 23 November 2022, date of publication 12 December 2022,
date of current version 30 December 2022.

Digital Object Identifier 10.1109/ACCESS.2022.3228386

RESEARCH ARTICLE

Improving Stability of Line Inspection Robot During Crossing Jumper Lines With a Centroid Adjustment Adjusting Mechanism

XIANG YUE[1,2], HONGGUANG WANG[2], YAN FENG[1], YONG TIAN[3], AND WEI WANG[1]

[1]College of Engineering, Shenyang Agricultural University, Shenyang 110866, China
[2]State Key Laboratory of Robotics, Shenyang Institute of Automation, Chinese Academy of Sciences, Shenyang 110016, China
[3]Department of Mechanical Engineering, College of Mechanical Electrical and Vehicle Engineering, Weifang University, Weifang 261061, China

Corresponding author: Wei Wang (syww@syau.edu.cn)

This work was supported in part by the National Natural Science Foundation of China under Grant 51605311, and in part by the Youth Program of Liaoning Education Department under Grant LSNQN202025.

ABSTRACT The stability of the inspection robot during crossing the jumper lines of the live lines of the 110kV power transmission is very important. In this study, a novel inspection robot was designed, equipped with a centroid adjusting mechanism to increase the stability during crossing the jumper line. The various obstacle crossing modes of the robot and the corresponding planning are designed. The dynamic modeling method for the rigid-flexible coupling of the robot in the flexible cable environment is studied, which helps to understand the influence of the robot on the transmission line in the environment. The simulation is carried out to analyze the deformation of the jumper line when the robot is on it. The results can be utilized to plan the motion to improve the robot's efficiency and stability when the robot crosses the jumper line.

INDEX TERMS Power transmission line, inspection robot, jumper line, obstacle-crossing.

I. INTRODUCTION

Power transmission lines inspection is to master the operation status of the line, find out the defects of power facilities and channels along the line in time, and provide data for transmission line maintenance. Compared with traditional manual inspection, transmission line inspection robots have the advantages of low inspection cost, high safety, high reliability, satisfactory inspection in close range, and easy operation [1], [2], [3], [4]. Power line robotics is now considered a part of the solution in the development of maintenance practices [5], [6].

Hibot company and Tokyo University of Technology in Japan have developed a teleoperation robot Expliner which can inspect and cross obstacles on 500kV and above transmission lines with a double-line structure [7]. The mechanism crosses the obstacles by adjusting the robot's center of mass position through the mechanical arm. The robot can cross straight-line towers and spacer bars. The disadvantage of the robot is that the structure is not compact, and the size is large. It is mainly used for multi-split conductors. The Quebec Hydropower Research Institute of Canada developed a robot LineDrone [8] that lands on a power line and then rolls along it to perform an inspection. The LineDrone can carry a significant payload directly onto energized lines and land there; several high-value inspection and maintenance tasks can be performed more efficiently. C. M. Shruthi1 [9] et. propose a novel robot mechanism that can cross tension towers through the jumper cables. The energy-based optimal trajectory from an initial position on the straight transmission line to the goal position on the jumper cable is designed by using the interior-point optimization technique for a ten-DoF dual robotic arm.

The Institute of automation of the Chinese Academy of Sciences and Shandong University of science and technology jointly developed a 110kV transmission line inspection robot [10]. The robot comprises of three flexible swing arm mechanisms and self-propelled driving devices, which combines the advantages of a multi-joint split mechanism and

The associate editor coordinating the review of this manuscript and approving it for publication was Xiaojie Su.

a wheel arm composite mechanism. The robot combines two motion modes of rolling movement and step creeping, ensuring a certain locomotion speed. The robot has significant overall stiffness, good attitude stability, and substantial obstacle-crossing ability. Shenyang Institute of Automation, the Chinese Academy of Sciences, proposed the AAPE series overhead transmission line inspection robots in 2002 [11], [12]. This robot generally employed a wheel-arm complex mechanism with substantial obstacle climbing ability and fast locomotion speed. The obstacle-climbing stability of the robot can be improved through the mass center adjusting mechanism. The robot can drive and inspect independently in the straight pole and tower line section and cross the tension tower by erecting auxiliary guide rails. These robots have obstacle-crossing ability, but there are still significant deficiencies in the ability to cross tension towers.

The line inspection robot travels along the overhead transmission line to complete the inspection operation and forms a rigid-flexible coupling system with the transmission wire. Therefore, the coupling effect between the robot and the working environment must be considered in the dynamic research of the line-patrol robot. Establishing the coupling dynamic model between the line-patrol robot and the flexible working environment and studying its coupling characteristics are the basis for realizing the fully automatic operation of the power line inspection robot.

The early research mainly explored the dynamic response of the suspended flexible cable itself. Irvine and Caughey [13] studied the linear free vibration theory of the flexible cable with slight sag fixed at both ends. Hagedorn and Schafer [14] studied the vibration theory of nonlinear suspended flexible cables. Subsequent researchers used these theories to study the dynamic response of high-altitude cables. Wu and Chen [15] used Lagrangian theory and the finite element method to establish the nonlinear dynamic model of the high-altitude flexible cable environment. Al-Qassab [16] used Hamilton's theory to construct the dynamic model of the high-altitude flexible cable environment. Williams [17] simplified the model by simplifying the cable car as a moving mass point to study the dynamic response of the moving load speed and mass to the suspending cable.

When the robot conducts inspection and maintenance operations, it needs multi-joint linkage. The robot is a complex dynamic system, the multi-joint motion will cause the vibration of the robot itself, which will be transmitted to the line through the coupling with the line. The dynamic equation of the Hamilton principle and finite element method was established by Zhang Tingyu et al. of Shanghai University. Using the Newton Euler method, transformation matrix and Jacobian matrix of the inspection robot, the kinematics equation, auxiliary coordinate transformation matrix, rigid flexible coupling dynamics model of the transmission line and the inspection robot are established.According to the rigid-flexible coupling dynamic model, the dynamic response of the robot inspection process to the transmission line under different working conditions was analyzed.

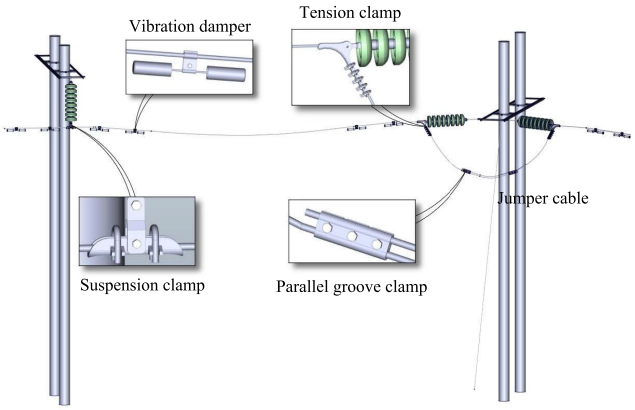

FIGURE 1. Environment schematic of 110kV transmission line.

Xiao Xiaohui et al. [18] of Wuhan University used the finite element method to establish a finite element model of a transmission line. They transferred the dynamic model of the transmission line to the transmission line inspection robot through boundary conditions. Using ADMAS as a platform, the simulation analysis of dynamic response under different working environments is carried out.

Most researches about the transmission line robot mainly focused on the autonomous control strategy, line fault detection, and maintenance methods. However, the research on the coupling relationship between the robot and the power transmission line was rarely studied. Because the transmission line is a flexible cable with variable stiffness, it is a challenge to establish the dynamic coupling model in the flexible cable environment [9], [19]. The computer programming and simulation is an effective method of simulating rigid, flexible coupling dynamics. Therefore, this paper analyzes the robot's configuration and reasonably plans the process of the robot when it crosses the jumper line according to the environmental characteristics. And the real-time environment model of the jumper line when the robot is crossing it is analyzed by simulation. Finally, the validity of the simulation model is verified through experiments.

II. ENVIRONMENT DESCRIPTION AND ROBOT CONFIGURATION ANALYSIS

A. ENVIRONMENT DESCRIPTION

According to the inspection task requirements for 110kV power transmission lines, the robot must travel along the power transmission line, navigate the obstacles, and carry the visible light camera and infrared camera to inspect the power transmission line and the auxiliary equipment.

The structure of the 110kV power transmission lines is very complicated, as there are straight towers, strain towers, conductors, OGWs, vibration dampers, and other electric power equipment. A general schematic of the 110kV transmission line is presented in Figure 1. There are many obstacles to conductors, such as vibration dampers, suspension clamps, strain clamps, and jumpers. The strain towers in the transmission grid are typical as they change the grid's direction due to terrain or avoidance of privately-owned land. A jumper is a short

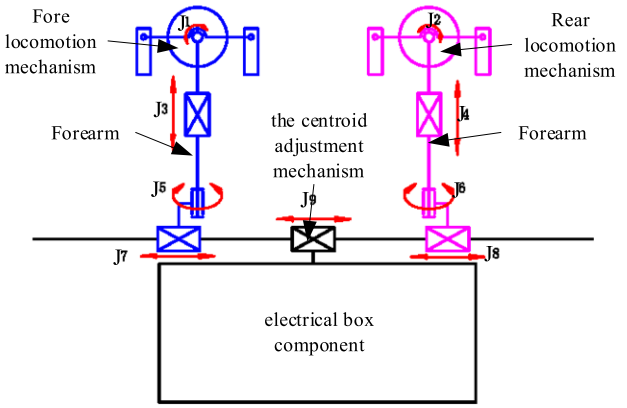

FIGURE 2. Schematic diagram of robot.

wire, not under mechanical tension, making an electrical connection between two separate sections of a line. Jumpers at strain towers are one of the most complex obstacles to traverse; they are flexible cables that are not as stiff as main spans and appear complex spatial curves. At the end of the jumper, it is nearly vertical, and its layout varies considerably from tower to tower. In order to accomplish the inspection task, the robot should be able to navigate the obstacle around straight-line towers and strain towers.

Because of the flexibility and un-tensioning, the posture of the jumper cable would change when the robot moves on it. Moreover, the jumper has many obstacles, such as strain and parallel groove clamps. The robot mechanism must be highly stable, simple, and have navigation capability. When gripping the jumper, the robot should not damage the cable. As the inspection tasks are carried out on energized lines, reducing the electromagnetic effect on the robot's performance is very important.

B. MECHANISM CONFIGURATION

The schematic diagram of the inspection robot is shown in Figure 2. The robot consists of two locomotion mechanisms, two arms, a centroid adjusting mechanism, and an electrical box. The locomotion mechanism ensures that the robot rushes on the cables. Each locomotion mechanism comprises of a wheel and two grippers (the fore-gripper and rear-gripper). J1 and J2 are revolving joints. When the robot navigates the strain clamp, the fore-gripper or the rear-gripper can rotate to grasp the jumper. Each arm includes a rotation joint and two translational joints. J3 and J4 are translational joints that provide a linear sliding movement for the forearm or the rear arm. They are designed to move the forearm and the rear arm upward and downward.

When the forearm or the rear arm hangs on the cable in the obstacle navigation process, the rear arm or the forearm is on or off the wire. With the help of the centroid adjusting mechanism, the robot's body can keep horizontal, which improves the stability of navigating obstacles. When the forearm hangs on the cable and the reararm is off the cable, the body of the inspection mechanism can turnabout the axes under the J5 and J6 driving and implement obstacle navigation. J7 and J8

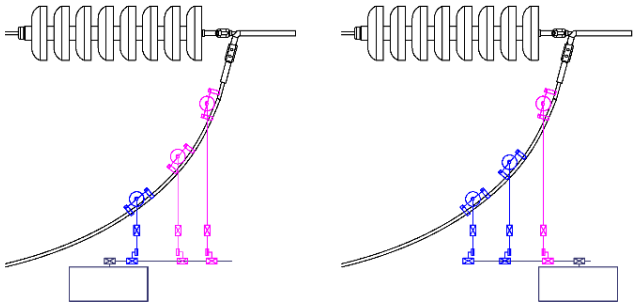

FIGURE 3. Inchworm maneuver.

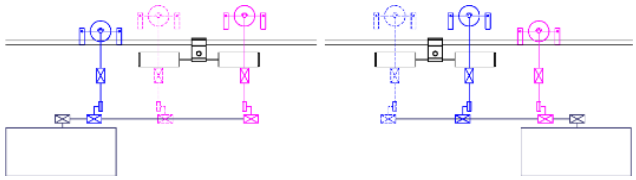

FIGURE 4. Brachiation maneuver.

are translational joints that drive the arm mechanism back and forth. J9 is a prismatic joint for centroid adjustment. The center of gravity can be located under the forearm or the rear arm by intentionally actuating the robot joints when navigating obstacles.

According to the configuration of the proposed inspection robot, obstacle navigation can be accomplished by two modes, namely, the brachiation mode and the inchworm mode.

As shown in Figure 3, when the inspection robot rolls on the line at a large angle, the process of obstacle navigation in the inchworm model is as follows:

Step 1: Make sure both wheels of the robot are on the cable. Then the rear locomotion mechanism grasps the cable, and the fore locomotion mechanism releases the cable;

Step 2: The centroid adjusting mechanism drives the forearm to move forwards and the forearm extents at the same time while the fore wheel is rolling on the cable;

Step 3: The inspection robot can roll on the prominent angle cable by repeating the above steps.

As shown in Figure 4, when the inspection robot encounters a damper, the process of obstacle navigation in brachiation maneuver mode is described as follows:

Step 1: The rear arm extends outwards until there is a gap between the damper and the rear arm;

Step 2: The centroid adjusting mechanism drives the rear arm to move forwards across the damper;

Step 3: With the help of the camera mounted on the rear arm, the cable is positioned, and the rear arm grasps the cable behind the navigated obstacle. The inspection robot can navigate obstacles by lifting two arms and repeating the abovementioned steps.

C. NAVIGATION PROCESS OF THE JUMPER

The characteristics of the jumper line itself make it difficult for the robot to cross. When the robot needs to cross the

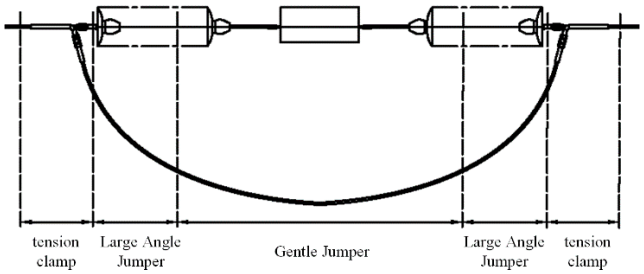

FIGURE 5. Three sections of the jumper line.

jumper line, the jumper line is divided into three sections according to the obstacle crossing methods required by the robot at different jumper positions, i.e., the tension clamp, the large-angle, and the gentle jumper. The obstacle crossing motion of the robot is planned in these three sections respectively to improve the obstacle crossing ability and efficiency, and the robot can pass through the jumper line smoothly. Figure 5 shows three different sections of the jumper line.

According to the 110kV transmission line environment analysis, jumpers represent the most challenging type of obstacles to traverse. The process of navigating strain clamps is a typical representative of the obstacle negotiation process. Taking a jumper obstacle as an example, the detailed descriptions of the tension clamp navigation sequence are as following:

(a) The robot stops in front of the obstacle to cross. The gripper of the forearm clamps firmly onto the conductor from above to ensure the robot's safety.

(b) The electrical box slides forwards so that the center of the gravity of the mechanism is located below the forearm. Then, the rear arm extends until there is enough clearance between the arm and the strain clamp, and the rear arm turns to move the rear locomotion mechanism away from the cable.

(c) The rear and forearms swing to move the closer mechanism into proximity to the jumper. The electrical box slides backward so that the center of the gravity of the mechanism is still located below the forearm. The rear arm rotates to align the rear gripper with the jumper, and the gripper clamps onto it, providing a new set of supports for the robot.

(d) The gripper of the forearm opens and moves away from the conductor.

(e) The rear and forearms swing to move the fore locomotion mechanism closer to the jumper.

(f) The forearm rotates to align the fore gripper with the jumper, and the gripper clamps onto it.

III. RIGID FLEXIBLE COUPLING DYNAMIC MODEL

The equations of motions of the jumper due to a moving robot could be derived from Hamilton's principle [20], [21]. Providing that the jumper suspended between two points at any arbitrary level. All dependent variables will be referenced to the stretched static shape described by the Cartesian coordinates $x(s)$ and $y(s)$, where s is the spatial variable measured along the cable length of the stretched configuration. The

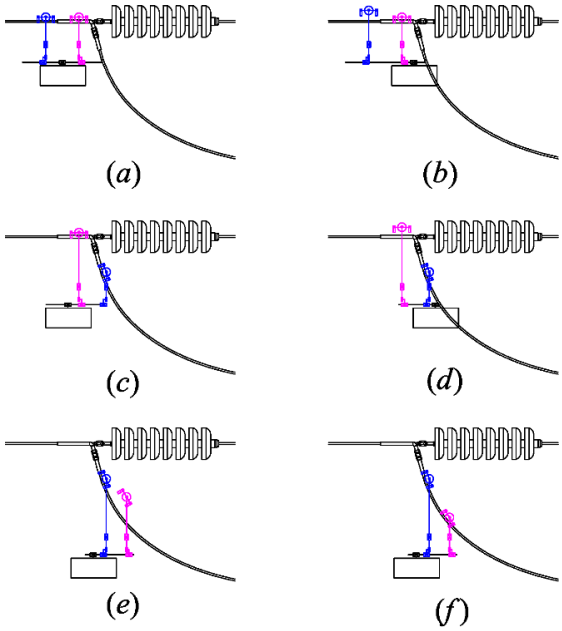

FIGURE 6. Process of crossing the jumper.

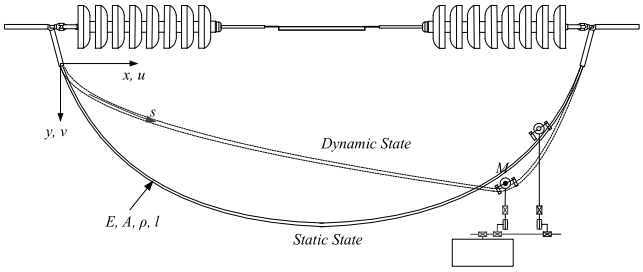

FIGURE 7. The static and dynamic configurations.

dynamic displacements in the longitudinal and transverse directions are described by $u(s, t)$ and $v(s, t)$, respectively, where t is time (Figure 7). Denoting the distance the robot has traveled along the cable as $s_o(t)$, its position vector $\hat{p}_o(t)$ can be represented as follows:

$$\hat{p}_o(t) = [x(s_o) + u(s_o, t)]\hat{\imath} + [y(s_o) + v(s_o, t)]\hat{\jmath}$$

where, $\hat{\imath}$ and $\hat{\jmath}$ are the fixed international unit vectors in the horizontal and vertical directions. For the general case of the characteristic motion of the moving mass, it is assumed that the mass has a local velocity $\mathrm{d}s_o(t)/\mathrm{d}t$ and a local acceleration $\mathrm{d}^2 s_o(t)/\mathrm{d}t^2$ along the arc length of the cable with a direction tangent to the cable at the location of the moving mass.

Then the velocity vector of the moving mass will be

$$\begin{aligned}\hat{v}_0(t) &= \frac{dp0}{dt} \\ &= \left(\frac{\partial u(s_0, t)}{\partial t} + \frac{ds_0}{dt}\left(\frac{dx(s_0)}{ds_0} + \frac{\partial u(s_0, t)}{\partial s_0}\right)\right)\hat{\imath} \\ &\quad + \left(\frac{\partial v(s_0, t)}{\partial t} + \frac{ds_0}{dt}\left(\frac{dy(s_0)}{ds_0} + \frac{\partial v(s_0, t)}{\partial s_0}\right)\right)\hat{\jmath}\end{aligned} \tag{1}$$

Equation (1) and the velocity vector of the cable at any arbitrary point on the cable, which is $\partial u(s,\ t)/\ \partial t\ \hat{l} + \partial v(s,\ t)/\ \partial t\ \hat{j}$, can be used to obtain the kinetic energy of the system as follows:

$$K = \frac{1}{2}\int_0^l \rho\bar{u}0 + \dot{v}ds + \frac{1}{2}\int_0^l M\delta(s - s_o(t)) \times \{(\dot{u} + \dot{s}_o(xI + uI)) + (\dot{v} + \dot{s}_o(y + v))\}ds \quad (2)$$

where, dot means partial differentiation concerning time, t, and the prime means partial differentiation concerning the space variable s, l is the cable length, ρ is the mass of the cable per unit length, M is the mass of the moving particle and $\delta(s)$ is the Dirac delta. If dS is the current arc length of the cable, the Lagrange strain $\varepsilon\ (s,\ t)$ becomes

$$\varepsilon\ (s,\ t) = \frac{dS - ds}{ds} = \sqrt{(x' + u')^2 + (y' + u')^2} - 1 \quad (3)$$

The potential energy can be written as

$$\Pi = \int_0^l \left(T\varepsilon + \frac{1}{2}EA\varepsilon^2 - \rho gv - Mg\delta\ (s - s_0\ (t))\ v\right) ds \quad (4)$$

where, T is the static cable tension and it is a function of s, g is the acceleration of gravity, E is the modulus of elasticity and A is the cross sectional area of the cable. Using Equation (2) and (4) in the Hamilton's principle:

$$\delta\int_{t_1}^{t_2} (K - \Pi)\ \mathrm{dt} = 0 \quad (5)$$

performing the variation on u and v and integrating by parts lead in (6), as shown at the bottom of the next page.

Note that the boundary terms of integration have been set equal to zero, which are

$$\int_0^l \left\{\left[\rho\dot{u} + M\delta\ (s - s_0)\ \left(\dot{u} + \dot{s}_0\ \left(x' + u'\right)\right)\right]\delta u + \left[\rho\dot{v} + M\delta\ (s - s_0)\ \left(\dot{v} + \dot{s}_0\ \left(y' + v'\right)\right)\right]\delta v\right\}\Big|_{t_1}^{t_2}\ ds = 0$$

$$\int_0^l M\delta\ (s - s_0)\ \left\{\left[\dot{u} + \dot{s}_0\ \left(x' + u'\right)\right]\delta u + \left[\dot{v} + \dot{s}_0\ \left(y' + v'\right)\right]\delta v\right\}\Big|_0^l\ dt = 0$$

and the following relation has been used

$$\frac{\partial\delta\ (s - s_0)}{\partial t} + s_0\frac{\partial\delta\ (s - s_0)}{\partial s} = 0$$

The boundary conditions of a fixed cable at its two ends are given by

$$u\ (0,\ t) = v\ (0,\ t) = 0 \quad u(l,\ t) = v(l,\ t) = 0 \quad (7)$$

and the initial conditions are

$$u(l,\ t) = \frac{\partial u\ (s,\ 0)}{\partial t} = 0 \quad v(l,\ t) = \frac{\partial v\ (s,\ 0)}{\partial t} = 0 \quad (8)$$

TABLE 1. Physical parameters of power transmission line.

Parameter		value
Sectional area	Aluminium (alloy) Aa /mm^2	181.34
	Steel As/mm^2	29.59
	total area St /mm^2	210.93
Elastic coefficient E/Pa		7.7×1010
Calculated breaking force T/N		3.152×105
Horizontal component of tension H/N		4.068×104
Diameter of transmission line D/mm		18.88
Horizontal distance between two adjacent towers L/m		522
Mass per unit length μ/(kg/m)		1.5955

IV. SIMULATIONS AND EXPERIMENTS

A. SIMULATION ANALYSIS

The jumper line at the strain tower is the most challenging obstacle for the inspection robot to cross. Because there is no tension at both ends of the jumper line, it is in a spatial flexible cable state under its gravity. The jumper line will be significantly deformed under the robot's action when the robot rolls. If the state of the jumper line cannot be predicted in advance, it will increase the difficulty of the robot to cross obstacle and reduce the obstacle crossing efficiency. Using the dynamic coupling model of the robot and the flexible cable environment established above, the real-time posture of the jumper line during crossing obstacle can be established. It provides a basis for the line grasping of the robot's locomotion mechanism and obstacle crossing planning, it significantly improves its efficiency.

The span of the jumper line in the simulation model in this paper is 3670mm, the wire diameter of the cable is 18.9mm, and the physical parameters of the standard steel cord aluminum strand are shown in Table 1.

The alternating crossing of two arms mainly completes the robot crossing the jumper line, and the centroid adjusting mechanism completes the attitude adjustment of the robot. The simulation process is to simplify the robot as a mass point acting on the position of the locomotion mechanism grasping the jumper line. Simulation analysis of the shape changes of the jumper line when the locomotion mechanism grasps different positions of the jumper line is shown in Figure 8.

Figure 9(a) is the simulation results obtained from the above algorithm. The changing shape of the jumper line obtained in the laboratory at the same position is shown in Figure 9(b). By comparing the simulation results with the laboratory test process diagram, it can be found that the simulation results are consistent with the test results, indicating the correctness of the simulation calculation.

Because there is no tension at both ends of the jumper line, it will produce great deformation when the robot rolls on the

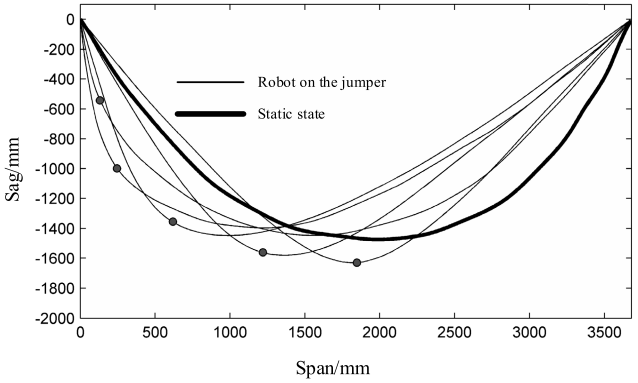

FIGURE 8. The shape of the jumper at different positions for the robot.

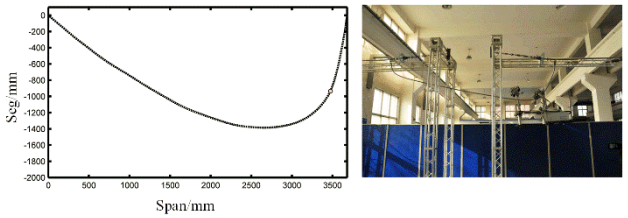

(a) Simulation analysis results (b) Test results

FIGURE 9. Comparison of test results and simulation results.

jumper line. The locomotion mechanism of the two arms is on line simultaneously to increase the contact area, reduce the jumper line's deformation, and improve the obstacle crossing efficiency. Figure 10 shows the shape comparison of the jumper line when the single arm and two arms are on line. The change of the jumper line when two arms are on line is significantly less than that of one arm on line, so the condition of one arm on line should be avoided as much as possible in obstacle-crossing planning. Therefore, the subsection planning of jumper line obstacle crossing is feasible and reasonable.

It can be seen from Figure 11 that when the robot rolls along the jumper line, the posture of the jumper line will change significantly, which will increase the difficulty of obstacle crossing and reduce the efficiency of obstacle crossing. In this study, the centroid position of the robot can be adjusted through the centroid adjusting mechanism to significantly reduce the deformation of the jumper line, increase the obstacle crossing efficiency and reduce the obstacle crossing difficulty.

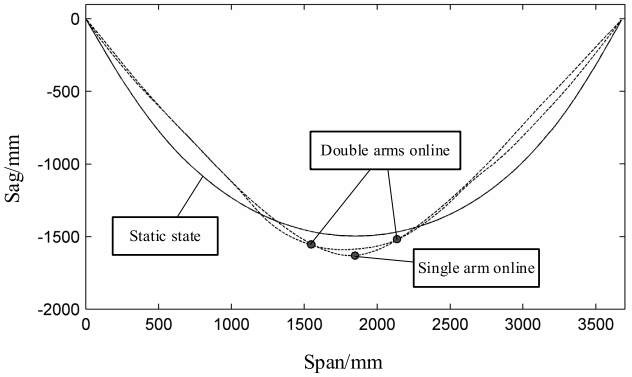

FIGURE 10. The jumper shape comparison with one arm and two arms online.

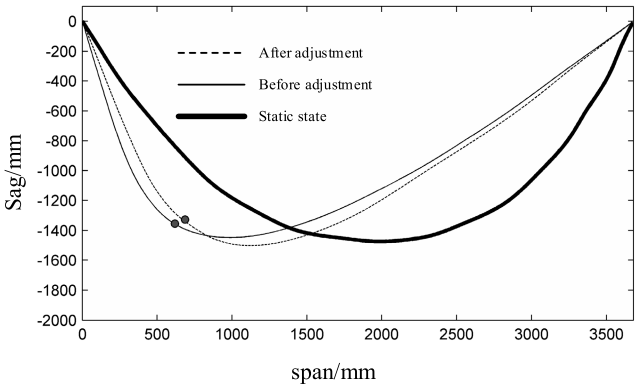

FIGURE 11. The deformation of the jumper line with the centroid adjusting mechanism.

B. EXPERIMENT VERIFICATION

To verify whether the designed robot can successfully cross the tension tower's jumper line, the robot's stability when crossing the obstacle, and the validity of the obstacle crossing planning of the jumper line, experiments have been designed and carried out under different working conditions. A high-voltage transmission line composed of a tension tower, a tangent tower, and cables is built up under laboratory conditions. The main power fittings are the jumper line, tension clamp, suspension wire, and shock hammer.

The experimental steps are as follows:

Step 1: Firstly, the online work of the robot is completed, the posture detection of the robot is started up and completed,

$$\int_{t_1}^{t_2}\int_{0}^{l}\left\{\left(\rho\ddot{u}+M\delta\left(s-s_0\left(t\right)\right)\left[\ddot{u}+2\dot{s}_0\dot{u}'+\dot{s}_0^2\left(x''+u''\right)+\left(x'+u'\right)\right]\right)\delta u\right.$$
$$+\left(\rho\ddot{v}+M\delta\left(s-s_0\left(t\right)\right)\left[\ddot{v}+2\dot{s}_0\dot{v}'+\dot{s}_0^2\left(y''+v''\right)+\left(y'+v'\right)\right]\right)\delta v$$
$$\left.+\frac{T+EA\varepsilon}{\varepsilon+1}\left[\left(x'+u'\right)\delta u'+\left(y'+v'\right)\delta v'\right]-\left[\rho+M\delta\left(s-s_0\left(t\right)\right)\right]g\delta v\right\}dsdt=0 \tag{6}$$

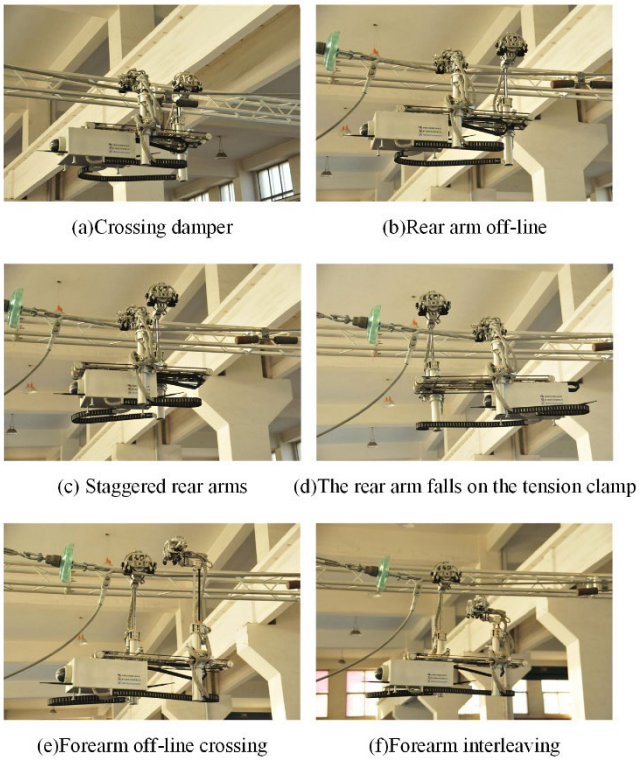

FIGURE 12. Experiments of strain clamp navigation.

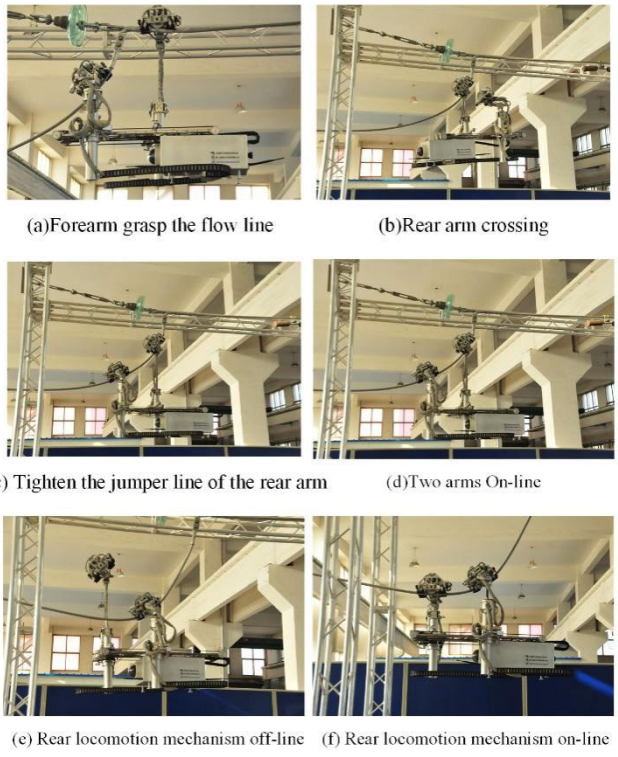

FIGURE 13. Experiments of large angle jumper navigation.

and the robot rolls along the line from one end of the transmission line.

Step 2: When the robot sensor detects the damper, the robot slowly approaches the damper, the forearm rises, and the rear-wheel drive robot moves forward to cross the obstacle. After the front arm completes the obstacle crossing, the rear arm rises, and the rear-wheel drive robot crosses the obstacle, as shown in Figure 12 (a).

Step 3: After crossing the damper, the robot continues to move forward. When the tension clamp is detected, the robot stops. Then the robot starts the brachiation maneuver to make the rear locomotion mechanism complete the clamping of the tension clamp to prepare for obstacle crossing, as shown in Figure 12 (b) ∼ (d).

Step 4: When the rear locomotion mechanism completes the grasping work, the forearm crosses the tension clamp in the brachiation maneuver. After crossing, the front locomotion mechanism clamps the jumper line, the centroid adjusting mechanism adjusts the robot centroid to reach the forearm, and the rear locomotion mechanism is disconnected. Figure 12 (e) ∼ (f) shows the obstacle-crossing process.

Step 5: The rear arm is off line, and the brachiation maneuver is adopted to cross the tension clamp. After the obstacle crossing is completed, the rear locomotion mechanism drops the line, and the obstacle crossing process of the tension clamp is completed, as shown in Figure 13 (a) ∼ (c).

Step 6: When the angle of the jumper line is too large, the robot cannot roll along the line employing two-wheel drive. The robot continues to cross the jumper line in the brachiation maneuver. Figure 13(d)∼(f) shows the obstacle-crossing process.

Step 7: When the inclination angle of the jumper line is within 24 degrees, the robot crawls along the jumper line employing two-wheel drive, as shown in Figure 14(a)∼(c)

Step 8: By detecting the real-time inclination angle of the jumper line, the robot rolls along the jumper line using different obstacle crossing modes and finally completes the obstacle crossing of the jumper line, as shown in Figure 14(d)∼(f).

The experimental results show that the robot can successfully cross the tension clamp and jumper line. In the real obstacle crossing process, the stability of the robot attitude can always be guaranteed through the robot centroid adjusting mechanism, and the deformation of the jumper line is reduced. Through proper obstacle crossing planning of the jumper line, the obstacle crossing efficiency has been dramatically improved to ensure the smooth realization of obstacle crossing. When the distance between two arms is 360mm, both the stability and efficiency of obstacle crossing can be considered.

The robot can successfully cross obstacles through experiments such as the hammer, tension clamp, and jumper line. The robot centroid adjusting mechanism can effectively reduce the change of robot posture and ensure the safety of robot obstacle crossing. According to the environmental model obtained from the simulation results, the robot can effectively and quickly cross obstacles, shorten the obstacle crossing time, and reduce the deformation of the jumper line and the damage to the line. The experimental results show that the simulation results are accurate and effective.

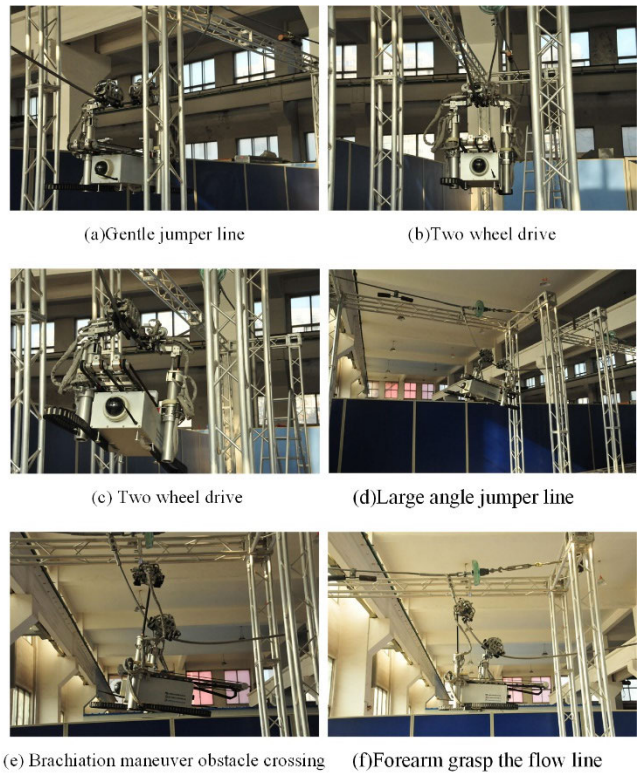

FIGURE 14. Experiments of gentle jumper navigation.

V. CONCLUSION

According to the transmission line's environmental characteristics and the inspection task's requirements, a novel transmission line inspection robot is designed. Using the various obstacle crossing modes of the robot, through the proper planning of the obstacle crossing of the jumper line, the obstacle crossing efficiency of the robot is improved, and the deformation of the jumper line is reduced. The simulation model can provide an accurate environment model for robot obstacle crossing, increasing the obstacle crossing efficiency of the robot, and realizing the whole line inspection by the robot.

REFERENCES

[1] Y. Song, H. Wang, and J. Zhang, "A vision-based broken strand detection method for a power-line maintenance robot," *IEEE Trans. Power Del.*, vol. 29, no. 5, pp. 2154–2161, Oct. 2014.
[2] S. Paul, D. Lee, K. Kim, and J. Chang, "Nonlinear modeling and performance testing of high-power electromagnetic energy harvesting system for self-powering transmission line vibration deicing robot," *Mech. Syst. Signal Process.*, vol. 151, pp. 1–18, Apr. 2021.
[3] A. Alhassan, X. Zhang, H. Shen, and H. Xu, "Power transmission line inspection robots: A review, trends and challenges for future research," *Int. J. Electr. Power Energy Syst.*, vol. 118, pp. 1–19, Jun. 2020.
[4] G. Rigatos, N. Zervos, P. Siano, M. Abbaszadeh, J. Pomares, and P. Wira, "A nonlinear optimal control approach for underactuated power-line inspection robots," *Robotica*, vol. 40, no. 6, pp. 1979–2009, 2022.
[5] W. Jiang, G. C. Ye, D. H. Zou, and Y. Yan, "Mechanism configuration and innovation control system design for power cable line mobile maintenance robot," *Robotica*, vol. 39, no. 7, pp. 1251–1263, 2021.
[6] P. L. Richard, N. Pouliot, F. Morin, M. Lepage, P. Hamelin, M. Lagace, A. Sartor, G. Lambert, and S. Montambault, "LineRanger: Analysis and field testing of an innovative robot for efficient assessment of bundled high-voltage powerlines," in *Proc. Int. Conf. Robot. Autom. (ICRA)*, Montreal, QC, Canada May 2019, pp. 9130–9136.
[7] M. Oyun-Erdene, B.-E. Byambasuren, E. T. Matson, and D. Kim, "Detection and localization of illegal electricity usage in power distribution line," *Multimedia Tools Appl.*, vol. 75, no. 9, pp. 4997–5012, 2014.
[8] P. Hamelin, F. Miralles, G. Lambert, S. Lavoie, N. Pouliot, M. Montfrond, and S. Montambault, "Discrete-time control of LineDrone: An assisted tracking and landing UAV for live power line inspection and maintenance," *19 Int. Conf. Unmanned Aircr. Syst. (ICUAS)*, Atlanta, GA, USA, Jun. 2019, pp. 292–298.
[9] C. M. Shruthi, A. P. Sudheer, and M. L. Joy, "Optimal crossing and control of mobile dual-arm robot through tension towers by using fuzzy and Newton barrier method," *J. Brazilian Soc. Mech. Sci. Eng.*, vol. 41, no. 6, pp. 1–25, 2019.
[10] X. A. Yue, H. G. Wang, and Y. Jiang, "A novel 110 kV power line inspection robot and its climbing ability analysis," *Int. J. Adv. Robot. Syst.*, vol. 14, no. 3, 2017, Art. no. 1729881417710461, doi: 10.1177/1729881417710461.
[11] H. Wang, F. Zhang, Y. Jiang, G. Liu, and X. Peng, "Development of an inspection robot for 500 kV EHV power transmission lines," in *Proc. IEEE/RSJ Int. Conf. Intell. Robots Syst.*, Taiwan, Oct. 2010, pp. 5107–5112.
[12] W. Guo, H. Wang, Y. Jiang, and P. Sun, "Visual servo control for automatic line-grasping of a power transmission line inspection robot," *Robot*, vol. 34, no. 5, pp. 620–627, 2012.
[13] H. M. Irvine and T. K. Caughey, "The linear theory of free vibrations of a suspended cable," *Proc. Roy. Soc. London A, Math. Phys. Sci.*, vol. 341, no. 1626, pp. 299–315, 1974.
[14] P. Hagedorn and B. Schäfer, "On non-linear free vibrations of an elastic cable," *Int. J. Non-Linear Mech.*, vol. 15, no. 4, pp. 333–340, 1980.
[15] J. S. Wu and C. C. Chen, "The dynamic analysis of a suspended cable due to a moving load," *Int. J. Numer. Methods Eng.*, vol. 28, no. 10, pp. 2361–2381, 1989.
[16] L. Wang and G. Rega, "Modelling and transient planar dynamics of suspended cables with moving mass," *Int. J. Solids Struct.*, vol. 47, no. 20, pp. 2733–2744, 2010.
[17] P. Williams, "Dynamics of a cable with an attached sliding mass," *ANZIAM J.*, vol. 47, pp. 86–100, Jun. 2006.
[18] X. Xiao, G. Wu, J. Wang, J. Xie, and S. Li, "The effect of joint movement on the nature, frequencies of transmission line inspection robot," in *Proc. 5th WSEAS Int. Conf. Signal Process., Robot. Automat.*, Madrid, Spain, Feb. 2006, pp. 329–334.
[19] X. Xiaohui, W. Gongping, and L. Sanping, "Dynamic coupling simulation of a power transmission line inspection robot with its flexible moving path when overcoming obstacles," in *Proc. IEEE Int. Conf. Autom. Sci. Eng.*, Scottsdale, AZ, USA, Sep. 2007, pp. 326–331.
[20] M. Al-Qassab, S. Nair, and J. O'Leary, "Dynamics of an elastic cable carrying a moving mass particle," *Nonlinear Dyn.*, vol. 33, no. 1, pp. 11–32, 2003.
[21] X. Zhou, S. Yan, and F. Chu, "In-plane free vibrations of an inclined taut cable," *J. Vib. Acoust.*, vol. 133, no. 3, 2011, Art. no. 031001.
[22] X. Yue, H. Wang, Y. Jiang, N. Xi, and J. Xu, "Research on a novel inspection robot mechanism for power transmission lines," in *Proc. IEEE Int. Conf. Robot. Biomimetics (ROBIO)*, Zhuhai, China, Dec. 2015, pp. 2211–2216.

XIANG YUE was born in Jining, Shandong, China, in 1986. He received the B.S. degree in mechanical design, manufacturing, and automation from the Shenyang University of Technology, Shenyang, Liaoning, China, in 2010, and the Ph.D. degree in pattern recognition and intelligent systems from the Shenyang Institute of Automation (SIA), Chinese Academy of Sciences, Shenyang, in 2017.

Since 2017, he has been a Lecturer at Shenyang Agricultural University, Shenyang. His research interests include electric powered robots and intelligent agricultural equipment.

HONGGUANG WANG received the B.Eng. degree in mechanical engineering from the Zhengzhou Institute of Technology, Zhenzhou, China, in 1986, the M.Eng. degree in mechanical engineering (mechanics) from Northeastern University, Shenyang, China, in 1993, and the Ph.D. degree in mechatronic engineering from the Graduate School, Chinese Academy of Sciences, Beijing, China, in 2008.

He is currently a Professor at the State Key Laboratory of Robotics, Shenyang Institute of Automation, Chinese Academy of Sciences, Shenyang. His current research interests include the analysis and synthesis of robot mechanisms, the mechanics of serial and parallel manipulators, as well as modular reconfigurable robots and autonomous mobile robots.

YAN FENG was born in Tongliao, Inner Mongolia, China, in 1998. He received the Bachelor of Engineering degree in agricultural engineering from Shenyang Agricultural University, in 2021, where he is currently pursuing the master's degree in agricultural engineering and information technology.

YONG TIAN was born in Weifang, Shandong, China, in 1988. He received the bachelor's degree in mechanical engineering from the Wuhan University of Technology, in 2012, and the Ph.D. degree in mechanical and electronic Engineering from the Shenyang Institute of Automation, Chinese Academy of Sciences, in 2019.

From 2019 to 2020, he worked as a Research Personnel of electronic control technology with Weichai Power Company Ltd. Since 2021, he has been working as a Lecturer with Weifang University. His research interests include collaborative robot configuration and dynamic characteristics analysis, power inspection robot system design, and agricultural robot system design.

WEI WANG was born in Shenyang, Liaoning, China, in 1979. He received the B.S. and master's degrees in mechanical engineering from Shenyang Agricultural University, Shenyang, in 2002 and 2005, respectively.

Since 2018, he has been a Professor at Shenyang Agricultural University. His research interests include green manure machinery, forestry, and fruit machinery.